Core-hole effects in x-ray-absorption spectra of fullerenes

Mats Nyberg, Yi Luo, Luciano Triguero, and Lars G. M. Pettersson
Department of Physics, University of Stockholm, P.O. Box 6730, S-113 85 Stockholm, Sweden

Hans Ågren
Department of Chemistry, Royal Institute of Technology, S-10044 Stockholm, Sweden

(Received 22 April 1999)

Near-edge x-ray-absorption fine-structure spectra of two fullerenes, C_{60} and C_{70}, have been simulated by means of density-functional theory techniques using ground-state Kohn-Sham orbitals, transition state potentials, or full core-hole potentials. The very good experimental agreement obtained when the full core hole explicitly is taken into account gives an indication of significant excitonic effects for the x-ray-absorption spectra of fullerenes. [S0163-1829(99)01935-9]

I. INTRODUCTION

Fullerenes and related materials have been intensively studied since the discovery of C_{60} in 1985.[1] Among various different experimental techniques[2] near-edge x-ray-absorption fine-structure (NEXAFS) measurements have been proposed to have special possibilities not only for the study of electronic and geometric conformations, but also—owing to the localization of the core hole to different atoms—to separate the roles of the chemically different carbons in the fullerene.[3–6,8,9] Simulations of the fullerene spectra also form a bridge towards the use of NEXAFS spectroscopy on carbon tubulites and related systems, such as carbon nitrides and boronites,[10] with outstanding material properties.[11] However, accurate first-principles calculations are not easily applied to such large systems, something that so far has hampered the analysis of the NEXAFS spectra.

Apart from the actual prediction of the experimental spectra, simulations of fullerene NEXAFS spectra are also interesting from the point of view of the formation of excitons. The magnitude of the excitonic effects in the fullerenes has actually been debated for quite some time.[8,12] Traditionally, excitons in solids are defined as electronic levels that are pulled down below the conduction band by the core hole and which then localize to the site of the core hole. In this respect, fullerenes evidently form an intermediate between diamond with sp^3 carbon and graphite with sp^2 carbons,[13] the spectrum of the former is well reproduced by the density of states of the unoccupied bands, while graphite shows a strongly excitonic π^* band. Other ways of identifying excitons refer to a localization parameter expressed as the ratio of the core-valence Coulomb interaction and the width of the conduction band (the unoccupied π band),[14] and to the comparison of NEXAFS spectra with inverse photoemission spectra, which are well described by the density of unoccupied states. Such comparisons for C_{60} and C_{70} have been conducted by Seki and co-workers.[8]

In the present work we take account of the fact that in the exciton interpretation of x-ray spectra, the energy levels shift and relocalize according to the creation of each particular core hole, while in the nonexcitonic interpretation the excited levels evolve according to the energy bands and density of states of the ground state. Thus experimental agreement for calculations with and without core holes, and possibly fractional core holes, should therefore give a good measure on excitonic effects. A related problem is the applicability of the equivalent cores $(Z+1)$ approximation, which is of computational significance owing to its efficiency.

In this work we use gradient-corrected density-functional theory (DFT) in order to calculate geometrical structures and x-ray-absorption spectra of C_{60} and C_{70}. Core-hole effects are examined through the use of different approaches: either using the full core-hole state, the transition potential approach with a half-occupied core hole, the $Z+1$ approximation, or the ground-state orbitals where the effect of the core hole is neglected.

II. THEORETICAL DETAILS

All the calculations have been done at the gradient-corrected DFT level. We have used the density-functional code deMon,[15] in which three different basis sets are used, namely, a normal orbital basis set and two auxiliary basis sets. The orbital basis set used in the present study in the calculations of spectra was the iglo-iii basis set of Kutzelnigg, Fleischer, and Shindler[16] for the excited carbon. A four-electron effective core potential[17] (ECP) was used to describe the other carbons. The use of ECP's helps the convergence of the core-hole state and has negligible effects on the accuracy of the calculated spectra. For the excited carbon, we use a double basis-set technique, where we use a normal orbital basis set in the minimization of the energy, and an added augmented diffuse basis set $(19s,19p,19d)$ which is used for construction of a static exchange (STEX) Hamiltonian.[18] The intensity of the spectral lines is obtained from the computed dipole transition matrix elements for excitations from the core (C $1s$) orbitals. These integrals were evaluated for one state, either the ground state, a transition potential (TP) state, including a half-occupied spin orbital, a full core-hole state, or a $Z+1$ state. The TP approach is known to provide reliable transition energies, and has also been seen to give good agreement with experiment for the intensities for many cases.[18,19] The approach of using a full core hole has been less exploited, mainly due to the fact that

the transition energies are not easily obtained in a single calculation as is the case in the TP approach. In the present study, the spectra calculated from the full core-hole approach are shifted so that the first spectral feature lowest unoccupied molecular orbital (LUMO) coincides with the calculated C(1*s*)-LUMO transition energy obtained through a ΔKS (Kohn-Sham) scheme, which involves the calculation of the energy difference between the ground state and the fully relaxed core-excited (1*s* to LUMO) state. The ionization potential (IP) is also calculated in a ΔKS scheme, where the energy is taken as the difference between the ground state and the fully optimized core-ionized state. A Gaussian function [full width at half maximum (FWHM) = 0.5 eV] is used for convoluting the spectra below the IP, while a Stieltjes imaging approach[20,21] is used to describe the spectra above the IP in the continuum. In all the calculations, we have used gradient-corrected functionals.[22] The choice of the gradient-corrected functionals seems not, however, to affect the calculated spectra in any visible manner, and almost identical results can be obtained using the simpler local-density approximation. The geometries are fully optimized at the same gradient-corrected DFT level using double-ζ plus double polarization (DZP) basis sets for all atoms.

III. RESULTS AND DISCUSSION

The experimental NEXAFS spectra of C_{60} and C_{70} have been reported by several groups.[3–6,8,9] Although the experimental conditions have been somewhat different, the overall spectral structures shown have been the same, with rich features below the ionization limit, and with most intensity gathered in the lowest valence region. This is in itself an indication of excitonic effects due to the interaction between the core hole and the excited electron.

With the X_α multiple-scattering (X_α-MS) local-density transition potential (TP) method, Wästberg *et al.*[12] could examine the effects of inclusion of a fractional core hole in the calculations of the x-ray-absorption spectrum of C_{60}. These calculations involved a transition state with a half-occupied core spin orbital.[19] By introducing a half core hole, a spectrum was obtained that was quite different from the spectrum given by the $Z+1$ approach using a semiempirical intermediate-neglect-of-differential-overlap (INDO) self-consistent-field calculation.[12] However, the agreement between theoretical and the experimental spectra was still quite limited.

The optimized bond lengths from the present DFT calculations on C_{60} and C_{70} are listed in Table I. Being a molecule with symmetry I_h, C_{60} has only one unique carbon atom, possessing two different bond distances to its neighbors. The calculated bond distances for C_{60}, (1.455 and 1.403 Å), are in excellent agreement with the experimental data[23] (1.45, 1.40 ± 0.015 Å).

Previous theoretical results for the bond distances of C_{60} have shown the necessity to include dynamical correlation in the calculational scheme. The best Hartree-Fock results published using a triple-ζ plus double polarization (TZP) basis set gave values of 1.448 and 1.370 Å,[24] while DFT calculations at the local-density approximation (LDA) level give results in closer agreement with experiment, 1.45 and 1.39 Å using Gaussian orbitals[25] for gas-phase C_{60}. For solid C_{60},

TABLE I. Bond distances (in Å) of C_{60} and C_{70} from the present DFT calculations compared to previous theoretical results and experiment, Refs. 23–28, 33. The eight bond distances for C_{70} are explained in Ref. 29.

System	This work	Previous theory	Experiment
C_{60}			
Bond 1	1.403	1.370,[a] 1.39,[b] 1.382,[c] 1.40,[d] 1.406[e]	1.40 ± 0.015
Bond 2	1.455	1.448,[a] 1.45,[b] 1.444,[c] 1.45,[d] 1.446[e]	1.45 ± 0.015
C_{70}			
Bond 1	1.460	1.451[f]	
Bond 2	1.408	1.375[f]	
Bond 3	1.455	1.446[f]	
Bond 4	1.400	1.361[f]	
Bond 5	1.455	1.457[f]	
Bond 6	1.443	1.415[f]	
Bond 7	1.430	1.407[f]	
Bond 8	1.476	1.475[f]	

[a]Hartree-Fock TZF basis set, Ref. 24.
[b]LDA, Gaussian basis sets, Ref. 25.
[c]LDA, solid C_{60}, Ref. 26.
[d]LDA, solid C_{60}, Ref. 27.
[e]MP2 calculations, Ref. 28.
[f]Hartree-Fock DZP basis set, Ref. 29.

LDA calculations gave the bond lengths 1.444 and 1.382 Å in a study by Troullier *et al.*,[26] and 1.45 and 1.40 Å in another study by Zhang, Yi, and Bernhole using plane waves.[27] Finally, calculations using the second-order Møller-Plesset (MP2) scheme for the geometry[28] yielded the values 1.446 and 1.406 Å. In summary, all the methods that include dynamical correlation give similar values for the bond lengths as compared to our results and experiments.

In Fig. 1 we show the optimized structure of C_{70}, where we also label the five symmetry inequivalent C atoms C1–C5 in accordance with previous work.[29]

The optimized geometry of C_{70} has D_{5h} symmetry, as has also been concluded from previous investigations.[29] The

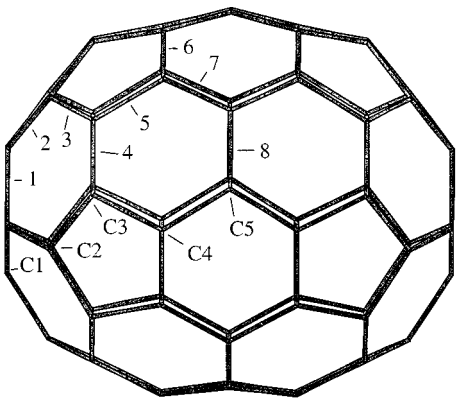

FIG. 1. Optimized structure for C_{70}. The five nonequivalent carbon atoms are here labeled C1–C5, and the eight different bonds are labeled with numbers 1–8.

TABLE II. 1*s* ionization potentials (IP) and 1*s*-LUMO excitation energies (eV) shown compared to available experimental data. The five different carbon atoms are denoted with indices C1–C5, as explained in Ref. 29.

System (No. of atoms)	IP (1*s*)	E_{exc} (1*s*-LUMO)
C_{60} (60)	289.56	284.55
C_{60} expt.	289.6[a,b]	284.45±0.05[c]
C_{70}^{C1} (10)	290.79	284.61
C_{70}^{C2} (10)	290.65	284.51
C_{70}^{C3} (20)	290.65	284.47
C_{70}^{C4} (20)	290.61	284.52
C_{70}^{C5} (10)	290.98	285.08

[a]Measured in solid phase.
[b]Reference 7.
[c]Reference 6.

bond distances for the five subgroups of carbon atoms (C1–C5) obtained from the present DFT calculations are presented in Table I. Our geometry is found to be slightly different from the previous theoretical Hartree-Fock result,[29] where the bond lengths are found to be in the range of 1.361 to 1.475 Å.

The ionization potentials, as well as the excitation energies for the C 1*s* to LUMO transition for C_{60} and C_{70} have been calculated using the ΔKS scheme, with the results shown in Table II. The excitation energies of C_{70} to the first valence state for the different carbon atoms are nonresolved at the given experimental resolution.[8] Our calculated results for C_{70} certainly confirm this observation. Not only is the first excitation energy referring to the different carbons unresolved, but the full NEXAFS spectra are remarkably alike for the C1–C4 group atoms. Only the C5 transitions are singled out, forming a higher excitation onset (explaining the experimental 285-eV structure) and a different NEXAFS spectrum, as shown in Fig. 4. This can be understood, since C5 is connected to three six-rings, while all the other carbons (C1–C4) are connected to two six-rings and one five-ring, similar to the case of C_{60}.

The experimental NEXAFS spectrum of C_{60} is known to have four discrete levels before the continuum,[4] as shown in Fig. 2, where the experimental data are taken from Ref. 30. Based on the ground-state calculation, the first three peaks can be assigned as t_{1u}, t_{1g}, t_{2u}, and h_g, where the latter two are energetically near degenerate. Within the frozen unoccupied density-of-states (UDOS) picture, one should anticipate that the third peak should have much higher intensity than the first two, which is in contrast to the picture provided by the experiment. The spectrum calculated from the transition potential (TP) approach, in which a half core hole is included, is slightly different from the UDOS picture. The intensity of the first peak, corresponding to t_{1u} within the TP approach is larger than that from UDOS. However, the third peak from the TP approach still has the largest intensity. The spectrum from the general DFT-TP approach is very close to the previous one obtained from X_α calculations.[12] However, it is clear that the results from the TP approach differ substantially from the full core-hole results for the calculated NEXAFS spectrum of C_{60}, and that a very good agreement

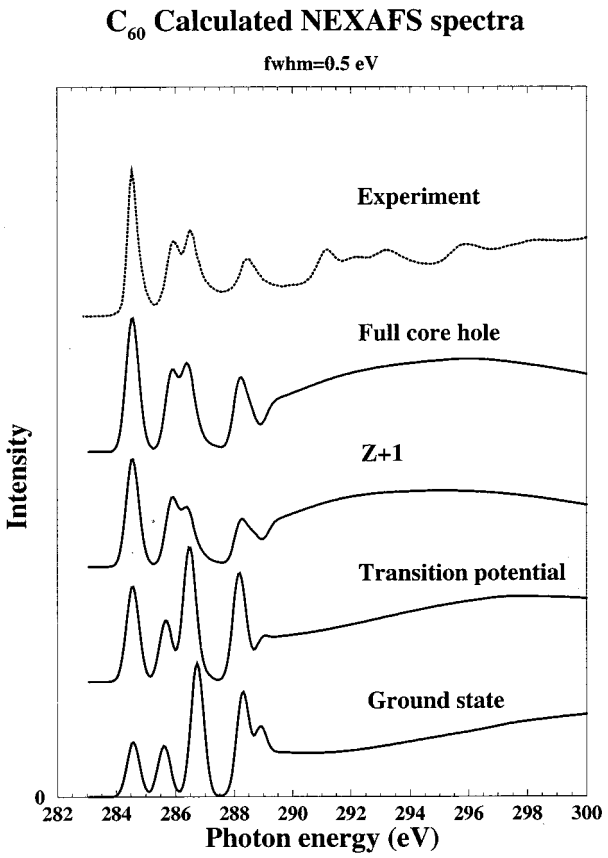

FIG. 2. Calculated NEXAFS spectra for C_{60}. The calculated spectra have been shifted so that the value of the excitation into the highest occupied molecular orbital (HOMO) corresponds to the calculated ΔKS transition energy (see the text for details). The experimental data are taken from Ref. 30.

with the experimental spectrum is obtained only by the latter results, see Fig. 2. The enhancement of the first feature is due to a localization of the lowest-lying valence state in the presence of the core hole, which thus indicates excitonic character.

The core-hole effects are further illustrated by the spectrum calculated from the $Z+1$ approximation: Most features in the spectrum are actually well described by the $Z+1$ approximation, only the composite middle 286-eV band is somewhat distorted in intensity. Physically, this indicates negligible effects of both the core-valence penetration and of the influence on the actual core—valence spin coupling on the electronic structure. Computationally, this means significant savings, since the $Z+1$ approximation corresponds to a closed-shell, ground-state-like calculation for which one can assume strict applicability of the Kohn-Sham theorem; it can, furthermore, be easily applied using any DFT or Hartree-Fock program.

Note that the use of Stieltjes imaging for C_{60} gives rise to a step structure at the IP, which is not present in the experimental spectrum. Furthermore, there are structures above the IP in the experiments which are not seen in the approach employed here. By considering the density of computed oscillator strengths in our underlying data for the Stieltjes imaging it is clear that much of the structure in the continuum region is smeared out and lost through the Stieltjes imaging

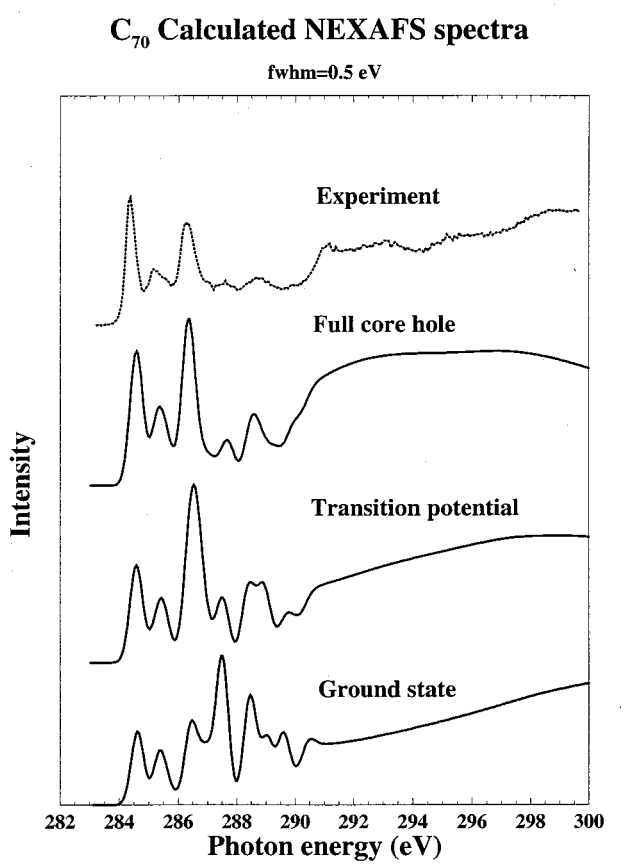

FIG. 3. Core-hole effects in the calculated C_{70} XA spectra, here illustrated by using the ground state, the transition potential state, and the full core-hole state; see the text for details. The experimental data are taken from Ref. 31.

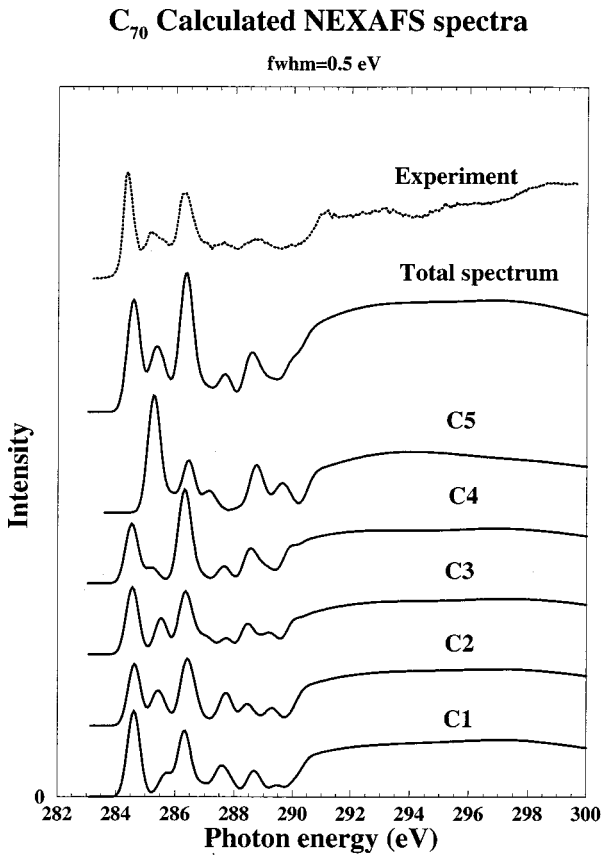

FIG. 4. Calculated NEXAFS spectra for C_{70} for the optimized structure. The individual components for the five different types of carbon, C1–C5, are shown together with the total spectrum. The total spectrum has been obtained by summing the five components scaled by their relative abundance. The ionization potential and the excitation energy into the first valence state was explicitly calculated in a ΔKS scheme.

procedure. How the treatment of the continuum should be improved in order not to lose information on shape resonances is presently not clear, and we refrain from discussing this energy region further in the present paper.

The excellent comparison of intensities with experiments for the valence states obtained from a full core-hole approach to C_{60} holds also for C_{70}. Due to the symmetry, the x-ray-absorption spectrum of C_{60} can be generated by calculating excitations from only one atom, while for C_{70} we need to calculate one atom out of each of the five groups, scale the spectra according to the relative abundance, and sum it all up. Figure 3 shows the calculated NEXAFS spectra for C_{70} using a ground state, a TP state, and a full core-hole state approach together with the experimental spectrum taken from Ref. 31. Similar to the case for C_{60}, the best comparison with experiment is obtained from the full core-hole approach. The difference between the core-hole and the transition potential approaches seems to be smaller than that for C_{60}, especially for the third π^* feature. It appears that the calculated intensity ratio between the first and the third feature is somewhat smaller than the one observed experimentally. One plausible explanation might be that the vibronic coupling is stronger in the region of the third feature due to the relatively high density of states present in this region. This would result in a broadening of this feature relative to the other peaks and a concomitant loss of peak intensity, just as observed from the experimental spectrum.

In comparing our calculated data (Fig. 4) to experiment,[4,32] we can relate all five pre-edge peaks seen experimentally to our calculated features. Although the direct evidence of the excitonic effects in the NEXAFS spectra of the fullerenes is best provided by the simulation of the actual spectrum, a population analysis of the electron localization of orbitals can also be informative. We find that peaks 1 and 3 originate from a molecular orbital localized on the excited carbon and its nearest neighbors for the four most common, C1–C4 (60 atoms in total) of the five different carbons, while peak 2 originates from the carbon that is least frequent, C5 (only ten atoms) (we label the features according to the order of appearance; peaks 1 and 5 are the lowest and highest, respectively, in energy). The localization effects can be seen as an increased Mulliken population on the excited atom and its nearest neighbors. For example, we have for peak 1 for C1 a calculated orbital population of 0.17 electrons in the core-hole state, but only 0.02 electrons for the ground state. Also the nearest neighbors get an increased population in this molecular orbital, a total of 0.32 electrons for the core-hole state as compared to 0.12 electrons in the ground state. The increased Mulliken population on the excited atom and its nearest neighbors in the presence of the core hole in the orbitals corresponding to features 1 and 3

constitutes an excitonic effect that is present for many extended systems, e.g., graphite.

IV. SUMMARY

We have shown that DFT calculations of NEXAFS spectra for the fullerene systems, here exemplified by C_{60} and C_{70}, give very good agreement with experimental high-resolution NEXAFS data. Geometry optimizations of these systems at the same level of theory result in good experimental agreement, indicating the possibility of analyzing these and similar systems theoretically from scratch. DFT in combination with a full core hole gives accurate estimations of oscillator strengths for the fullerenes that have valence orbitals which are highly delocalized, and for which excitonic effects might occur. In fact, the superiority of the full core-hole calculations over the transition potential and, in particular, the ground-state calculations, indicates that excitons indeed are important in the formation of the x-ray-absorption states in the fullerenes. The good agreement also sheds optimisim on the application of computations of the present kind for taking on ''real issues'' concerning fullerenes, such as, e.g., the isomeric proportions of the larger fullerenes, for which highly resolved NEXAFS spectra now become available.[9]

[1] H. W. Kroto, J. R. Heath, S. C. O'Brien, R. F. Curl, and R. E. Smalley, Nature (London) **318**, 162 (1985).

[2] Amos B. Smith, III, *Fullerene Chemistry* (Pergamon, Oxford 1996).

[3] C. T. Chen, L. H. Tjeng, P. Rudof, G. Meigs, J. E. Rowe, J. Chen, Jr., J. P. McCauley, A. B. Smith III, A. R. McGhie, W. J. Romanow, and E. W. Plummer, Nature (London) **352**, 603 (1991).

[4] L. J. Terminello, D. K. Shuh, F. J. Himpsel, D. A. Lapiano-Smith, J. Stöhr, D. S. Bethune, and G. Meijer, Chem. Phys. Lett. **182**, 491 (1991).

[5] H. Shinohara, H. Sato, Y. Saito, K. Tohji, I. Matsuoka, and Y. Udagawa, Chem. Phys. Lett. **183**, 145 (1991).

[6] P. A. Brühwiler, A. J. Maxwell, P. Rudolf, C. D. Gutleben, B. Wästberg, and N. Mårtensson, Phys. Rev. Lett. **71**, 3721 (1993).

[7] A. J. Maxwell, P. A. Brühwiler, D. Arvanitis, J. Hasselström, and N. Mårtensson, Chem. Phys. Lett. **260**, 71 (1996).

[8] K. Seki, R. Mitsumoto, T. Araki, E. Ito, Y. Ouchi, K. Kikuchi, and Y. Achiba, Synth. Met. **64**, 353 (1994).

[9] R. Mitsumoto, H. Oji, I. Mori, Y. Yamamoto, H. Shinohara, K. Seki, K. Umishita, S. Hino, S. Nagase, K. Kikichi, and Y. Achiba, J. Phys. IV **7**, 525 (1997).

[10] M. Nyberg, L. Triguero, L. G. M. Pettersson, T. Sikora, and R. Räty (unpublished).

[11] M. L. Cohen, Phys. Rev. B **32**, 7988 (1985).

[12] Bo Wästberg, S. Lunell, C. Enkvist, P. A. Brühwiler, A. J. Maxwell, and N. Mårtensson, Phys. Rev. B **50**, 13 031 (1994).

[13] G. Comelli, J. Stöhr, C. J. Robinson, and W. Jark, Phys. Rev. B **38**, 7511 (1988).

[14] F. Kh. Gelmukhanov and H. Ågren, J. Phys. B **28**, 3699 (1990).

[15] M. E. Casida, C. Daul, A. Goursot, A. Koester, L. G. M. Pettersson, E. Proynov, A. St-Amant, D. R. Salahub, DEMON-KS version 4.0 (deMon Software, 1997).

[16] W. Kutzelnigg, U. Fleischer, and M. Shindler, *NMR-Basic Principles and Progress* (Springer-Verlag, Heidelberg, 1990), Vol. 23, p. 165.

[17] L. G. M. Pettersson (unpublished).

[18] L. Triguero, L. G. M. Pettersson, and H. Ågren, Phys. Rev. B **58**, 8097 (1998).

[19] J. C. Slater, *Quantum Theory of Molecules and Solids Vol. IV* (McGraw-Hill, New York, 1974).

[20] P. W. Langhoff, *Electron-Molecule and Photon-Molecule Collisions* (Plenum, New York, 1979).

[21] P. W. Langhoff, *Theory and Application of Moment Methods in Many-Fermion Systems* (Plenum, New York, 1980).

[22] A. D. Becke, Phys. Rev. A **38**, 3098 (1988).

[23] C. S. Yannoni, P. P. Bernier, D. S. Bethune, G. Meijer, and J. R. Salem, J. Am. Chem. Soc. **113**, 3190 (1991).

[24] G. E. Scuseria, Chem. Phys. Lett. **176**, 423 (1991).

[25] B. I. Dunlap, D. W. Brenner, J. W. Mintmire, R. C. Mowrey, and C. T. White, J. Phys. Chem. **95**, 5763 (1991).

[26] N. Troullier and J. L. Martins, Phys. Rev. B **46**, 1754 (1992).

[27] Q.-M. Zhang, J.-Y. Yi, and J. Bernhole, Phys. Rev. Lett. **66**, 2633 (1991).

[28] M. Haser, J. Almlöf, and G. E. Scuseria, Chem. Phys. Lett. **181**, 497 (1991).

[29] J. Baker, P. W. Fowler, P. Lazzeretti, M. Malagoli, and R. Zanasi, Chem. Phys. Lett. **184**, 182 (1991).

[30] Y. Luo, H. Ågren, F. Kh. Gelmukhanov, J. H. Guo, P. Skytt, N. Wassdahl, and J. Nordgren, Phys. Rev. B **52**, 14 479 (1995).

[31] J. H. Guo, P. Skytt, N. Wassdahl, J. Nordgren, Y. Luo, O. Vahtras, and H. Ågren, Chem. Phys. Lett. **235**, 152 (1995).

[32] E. Sohmen, J. Fink, and W. Krätschmer, Z. Phys. B **86**, 87 (1992).

[33] G. E. Scuseria, Chem. Phys. Lett. **180**, 451 (1991).